Proceedings of Global Power and Propulsion Society
ISSN-Nr: 2504-4400
GPPS Chania22
18th–20th September, 2022

www.gpps.global

GPPS-TC-2022-0066

Influence of shafts flexibilities in Static Transmission Error estimation

Fabio Bruzzone
Politecnico di Torino, GeDy TrAss
fabio.bruzzone@polito.it
Torino, Italy

Carlo Rosso
Politecnico di Torino, GeDy TrAss
carlo.rosso@polito.it
Torino,Italy

ABSTRACT

Geared transmissions are prone to harmful vibrations and annoying noise emissions. The sources of excitation of those vibrations are many and different in nature, starting from torque fluctuations from the engine or the unsteady aerodynamics in wind turbines for example. However, the main source of excitation comes from an intrinsic characteristic of meshing gears and is the time varying mesh stiffness which is generated by the transmission error. Several flexibilities can be accounted in the calculation of the transmission error depending on the complexity of the model employed. In this paper the importance of including shafts flexibilities is highlighted. A nonlinear semi-analytical model is applied to the study of a simple test case with and without the misalignment caused by the inflection of the shafts under load and several results, such as the static transmission error and the contact pressure maps, are shown and discussed.

INTRODUCTION

Load and stiffness fluctuations are the main source of excitation and cause of failure in geared transmissions Abersek et al. (2004); Prasil and Mackerle (2008); Bruzzone and Rosso (2020). The Japanese school in the end of the twentieth century highlighted the complex dynamic features of gears analyzing their torsional behavior including other sources such as profile errors or modifications Sato et al. (1983); Umezawa et al. (1984, 1986); Kubo et al. (1986); Yang and Lin (1986). The Dynamic Factor (DF) was used to explain certain types of failures Ozguven and Houser (1988) by comparing the dynamic loads in operation with those under static conditions. Vibrations and impacts can certainly be traced back to variations in the input torque depending on the machine characteristics Kadmiri et al. (2011); Bel Mabrouk et al. (2017); Garambois et al. (2017), but the Time-Varying Mesh Stiffness (TVMS) was quickly found to be a key player Harris (1958). Indeed the stiffness of an engaging gear pair generates self-excited vibrations which led many researches in the study of the Transmission Error (TE). Several methods have been proposed, starting from integral approaches Weber (1949); Weber and Banaschek (1953) or discrete ones Cornell and Westervelt (1978); Cornell (1981). Experimental methods were also proposed to study the Static Transmission Error (STE) Chi et al. (2007); Raghuwanshi and Parey (2016, 2018) while others included mounting and manufacturing deviations to estimate the Manufacturing Transmission Error (MTE) Wei et al. (2011); Zhang et al. (2013); Inalpolat et al. (2015); Wang and Zhang (2017). Finite Element (FE) models were obviously proposed as well, but its computational effort and difficulty to set up made it applicable to limited aspects such as tooth root stresses and its structural behavior Deng et al. (2003); Lin et al. (2007); Pedersen and Jorgenses (2014), crack propagation Ural et al. (2005); Chaari et al. (2009); Qin and Guan (2014); Cura et al. (2015, 2014) or generally as a validation tool for other proposed models. Hertzian theory Hertz (1895) of cylinder-to-cylinder contact is generally employed to model the contact between engaging flanks, simplifying several key aspects of the gears, such as the continuously varying curvature and the presence of sharp edges. When contact is not neglected it is generally introduced as an addition to the elastic behavior of the mating teeth, but still under Hertz's hypotheses Hu and Chen (2003); Wang and Howard (2006); He et al. (2007); Y. Tesfahuneng et al. (2010); Nikolic et al. (2012) while other works included non-Hertzian properties, but neglected the flexibility under load of the teeth. Hybrid approaches coupling a FE model with a Semi Analytical (SA) contact model have also been proposed Parker et al. (2000) with great success. In Bruzzone et al. (2021*b*) a combination of some of the presented approaches will be used to accurately estimate the STE and the contact conditions including the influence of the micro-geometrical modifications of the teeth flanks both along its height and along the facewidth. In addiction a technique for taking into account the flexibilities of other gearbox components was developed and is here presented.

METHODOLOGY

In this paragraph a synthesis of the methodology described in Bruzzone et al. (2021*b*) is reported. The goal of this process is to compute the Static Transmission Error in mating gears by considering the possible tooth profile modifications and the different levels of applied torque. This methodology considers a Semi Analytical model based on Cornell (1981) in order to determine the stiffness of the different mating pairs. No a priori assumptions is made regarding the location of the contact point as well as the number of mating pairs bearing the load and the load sharing among them. The rigid body kinematics are only employed as the first tentative guess for a nonlinear iterative scheme in which also the working pressure angle is dependent on the deformation. A natural equilibrium condition is sought for the location, number and load intensity acting on the contact points found by a surface-to-surface intersection algorithm.

As detailed in Bruzzone et al. (2021*a*) during engagement the elastic deformation of the meshing teeth pairs causes a relative sliding between the contacting flanks causing a subsequent shift of the contact point where the load should be applied. Since the contact point changes, the stiffness of the engaged pair changes thus also altering the load sharing characteristics. For those considerations an iterative approach has been applied starting from the rigid contact conditions and then updating the contact point, the load of each teeth pair and the number of pairs in contact. At the k^{th} iteration using the updated contact point for the j^{th} pair the load sharing coefficient is computed by Ma et al. (2015)

$$C_{k,j} = \frac{k_j}{\sum_{i=1}^{N} k_i} \left(\frac{1 + \sum_{i=1}^{N} k_i \tilde{E}_{ji}}{F} \right) \tag{1}$$

where the relative displacement is $\tilde{E}_{ji} = \delta_j - \delta_i$ and k_j is the j^{th} teeth pair stiffness while the meshing force is $F = T/r_b = \sum_{j=1}^{N} F_j$ where T is the total torque to be transmitted and r_b is the base radius of the pinion. A natural equilibrium condition is reached when the contact points of the different engaging pairs are in a stable position as well as the load sharing coefficients, meaning

$$\frac{x_{k,j} - x_{k-1,j}}{x_{k,j}} < \varepsilon_x \wedge \frac{y_{k,j} - y_{k-1,j}}{y_{k,j}} < \varepsilon_y \wedge \frac{z_{k,j} - z_{k-1,j}}{z_{k,j}} < \varepsilon_z \wedge \frac{C_{k,j} - C_{k-1,j}}{C_{k,j}} < \varepsilon_C \tag{2}$$

where $x_{k,j}$, $y_{k,j}$, $z_{k,j}$ are the coordinates of the contact point of the j^{th} engaging pair at the k^{th} iteration and ε_x, ε_y, ε_z and ε_C are tolerance values generally equal to $10^{-2}\%$. Once equilibrium is reached a detailed contact model is used to study the contact between the so obtained deformed profiles.

A three-dimensional non-Hertzian contact model is employed to correctly model the interaction between the meshing flanks. Side and tip mirroring corrections are introduced to relieve the stresses on the free surfaces of the finite-length bodies in contact allowing accurate representation of the varying curvature and discontinuities of the flanks. The generation of the tooth geometry by using Tooth Profile Modifications (TPM) is introduced, an example is depicted in Figures 1a and 1b. To account for the continuously changing curvature of the flanks, the effects of the profile modifications and discontinuities such as the gear edges and tip, a detailed numerical rough frictionless non-Hertzian contact model is implemented. The contact problem is usually stated as the Hertz-Signorini-Moreau problem Johnson (1985); Kalker (1990); Wriggers (2002) The proposed contact model has been derived from the elastic half-space theory and hence implies that in any transverse section a plane state of deformations is respected. However, when one or both the contacting bodies have finite length, it is evident that the end faces are to be treated as free boundaries, but in a plane state of deformations two shear stresses and a normal stress would be present at the free faces. To remove those unrealistic stresses a correction based on mirror pressure distribution is introduced.

In order to consider the misalignment, a consideration has to be made. The misalignment can be due to manufacturing process or to the elastic deformation of the gearbox components. The proposed methodology was developed to take into account both, but the second one is the most important in design phase, because, no indication is present with respect to the production and assembly process. Misalignment is then considered as an imposed displacement of the gear pair. If manufacturing error is considered, the imposed displacement is introduced according to the experimental evaluation. If the deflection under load is taken into account, the influence of the torque and the stiffness of the gearbox has to be considered. To do this, the compliance of the shafts, bearings and casing must be considered and the meshing force will be applied on each gearing. In such a way, the 3D displacement of the gear pair is evaluated as the deformation of the shafts where gears are mounted and that value is used to move the position of the gear center, thus altering the position of the contacting flanks in a $Oxyz$ cartesian reference frame. After this static calculation and the application of the so computed displacement to the positions of the gears, the calculation of the Static Transmission Error is performed as previously described. The compliances of the gearbox elements are taken into account by modelling the shafts as Timoshenko beams, the bearings as linear springs depicted by 12 x 12 diagonal matrices and the casing using the actual CAD model and the consequent FE model statically reduced to the connection nodes. A shaft is connected to the connection points on the casing by means of the bearing matrices and to the other shafts by means of the gears. The gear connection can be described according to gear theory Litvin (1994). Two notable points can be defined: T_1, the tangent point between the Line Of Action (LOA) and the base circle of the gear, and C, the pitch point. As shown in Figure 2, a rigid link is created between the node T_1 and the C node, in order to guarantee connection and motion along the line of action. The same approach describes the gear. The

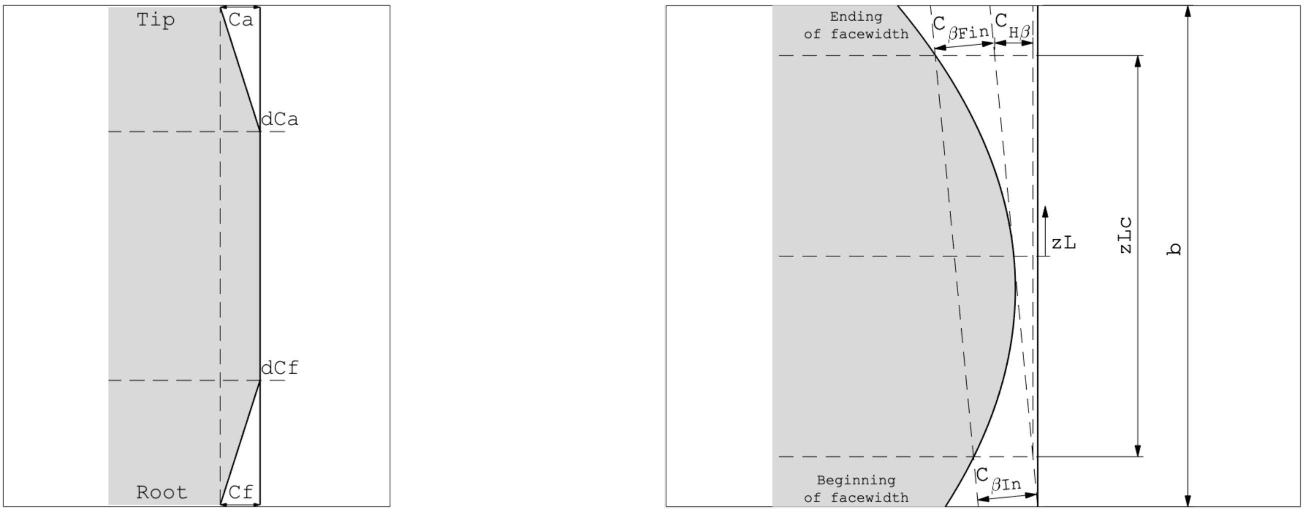

(a) Tip and root relief

(b) crowning

Figure 1 Tooth profile modifications

elastic displacements (u, v, w) and rotations $(\theta_x, \theta_y, \theta_z)$ are obtained from a static analysis at each angular position considered in the mesh cycle using standard FE procedures. The misaligned flank coordinates x', y', z' are obtained starting from the rigid coordinates x, y, z as

$$[x', y', z']^T = [x+u, y+v, z+w]^T \cdot \mathbf{R}_{\theta_x} \cdot \mathbf{R}_{\theta_y} \cdot \mathbf{R}_{\theta_z} \tag{3}$$

where $\mathbf{R}_{\theta_i}$ is a rotation matrix around the i axis. A flowchart of the numerical procedure is visualized in Figure 3.

RESULTS AND DISCUSSION

In this paragraph a comparison of the results obtained with the proposed approach considering the misalignment and different combinations of profile modifications is shown. The tested gears are visible in Figure 4 and their data are listed in Table 1. The gears are supported by two identical solid shafts, each with a diameter of $20mm$, length of $140mm$ and supported at a distance of $40mm$ from the closest constraint on the shaft loaded with a torque $T = 250Nm$. The shafts in the present example are reasonably thin in order to magnify some of the results. As a starting point the nominal tooth profiles will be analyzed and later profile modifications of different intensities will be applied. The first quantity that can be analyzed in this case is the STE which is visible in Figure 5. In this figure the black curve displays the STE obtained without considering the flexibility of the shafts, while the red one includes the influence of this compliance as described in the previous section. Only the Peak To Peak (P2P) value is shown because the flexible rotation θ_z of the shaft around its rotational axis have changed the mean value of the STE. It is evident that including the effect of the misalignment changes its shape and the amplitude of variation. The tested gear pair has a total contact ratio of 2.45 and indeed the rigid case the STE has a small drop in the triple contact zone, but it is otherwise smooth and with low variance. Including the misalignment dramatically increases the difference between the minimum and maximum deformation of the teeth, while also generating some spikes in the contact. This difference is also evident in the contact pressures along the flank obtained through the non-Hertzian contact algorithm as visible in Figure 6. Without profile modifications the contact patch of Figure 6a shows important pressure peaks at the tip and at the base of the flank. This is due to the fact that the tips of the gears are modeled as sharp, and hence with very sudden curvature change causing high pressures. In Figure 6b the same results with the inclusion of the misalignment is shown. The pressure peaks at the tips are even more enhanced reaching peaks of around $6000MPa$ and furthermore a shift to the left can be greatly appreciated. Due to the inflection of the shafts the contact is not in the ideal rigid position and hence the gears are forced to mate only on a portion of the surface of the flank, reducing the total contact area and increasing the mean pressure also in the center of the facewidth, and possibly causing failures if not accounted for.

Next, the first set of profile modifications is introduced on the same gears. The TPM applied in this case is a combination of linear tip relief and parabolic crowning whose data are listed in Table 2 referring to the nomenclature visible in Figure 1. In this case the P2P of the STE is visible in Figure 7 and shows similar features to the previous analysis. In the rigid shafts model the triple contact zone is reduced since some of the material of the gears has been removed, shorting the path of contact. The misaligned model shows again higher amplitude of oscillations during the mesh cycle, as well as important variations from one angular position to the next, which would cause severe vibrations in operation. The introduction of this first set of profile modifications significantly reduces the tip corner contact problem as visible in Figure 8 for both approaches. In the rigid case the problem is almost solved even with this light modification and it is visible that the contact pressure is more concentrated towards the center due to the presence of the face crowning on both mating gears.

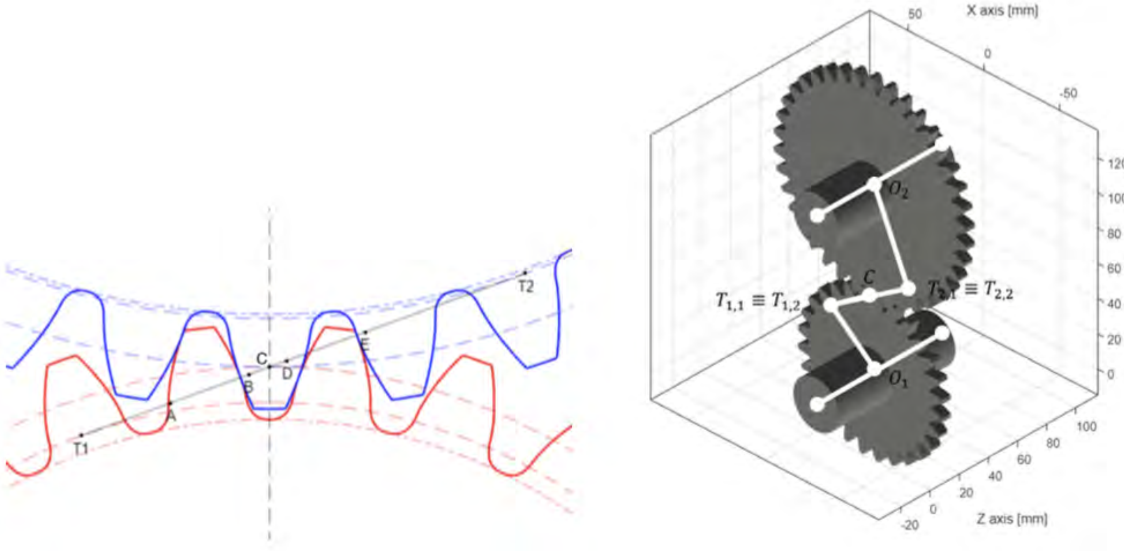

Figure 2 Scheme for links between shafts that depicts the gear set

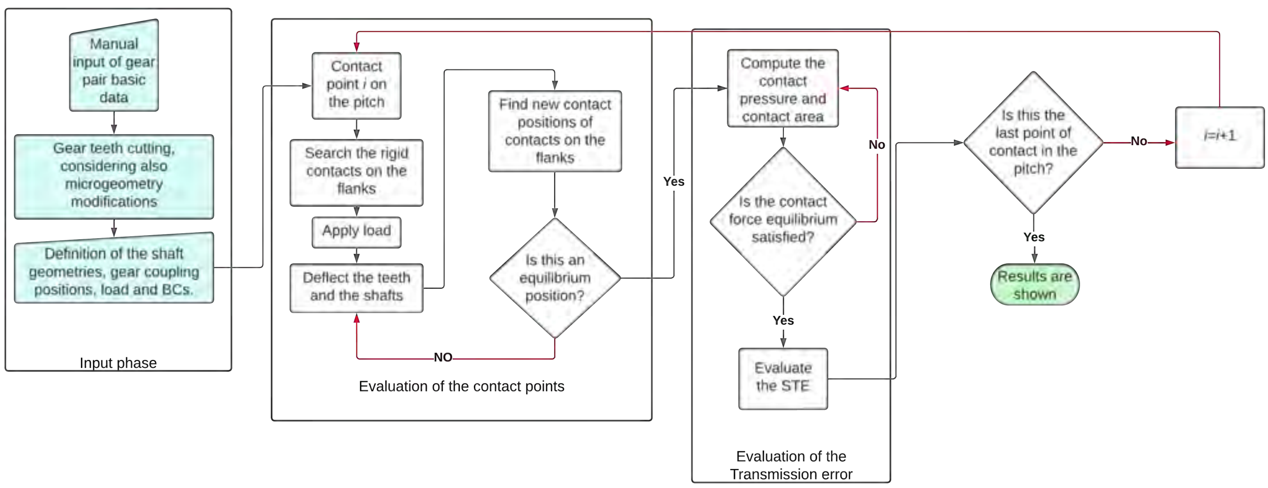

Figure 3 Flowchart of the numerical procedure

Considering the influence of misalignment some stress concentration region is still present at the tip, and also in this case the contact is shifted causing an increase of the pressure in the middle of the facewidth of around 12% with respect to the rigid case.

Table 1 Mating gear main parameters.

	Quantity	Units
Pinion number of teeth	28	
Gear number of teeth	53	
Module	3.175	mm
Pressure angle	20	$^\circ$
Helix angle	20	$^\circ$
Face width	26	mm
Reference Rack	ISO 53/A	
Shaft Young's modulus E	$2 \cdot 10^5$	MPa

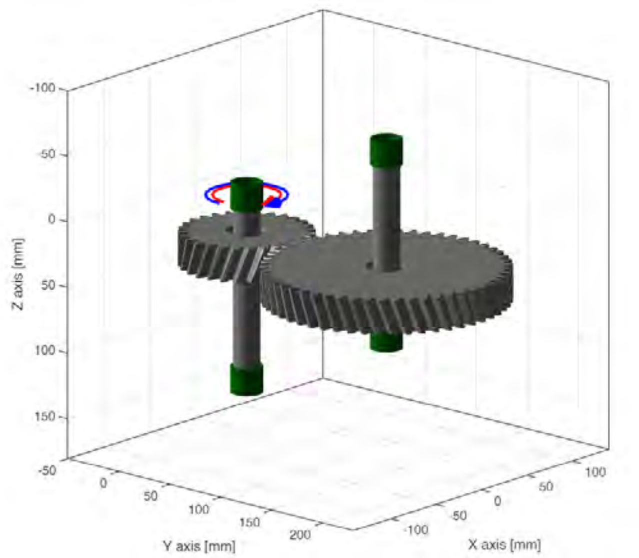

Figure 4 Tested gears.

Table 2 First set of profile modifications, linear tip relief and crowning.

Parameter	Pinion	Gear
dCa	$99.5mm$	$183.5mm$
Ca	$4\mu m$	$4\mu m$
$C\beta In$	$3\mu m$	$3\mu m$
$C\beta Fin$	$3\mu m$	$3\mu m$

A more aggressive set of profile modifications can be applied to further improve the mating of the gears and the parameters used are listed in Table 3 for this second test. This time the crowning is paired with a parabolic tip relief, which removes the material more smoothly from the flank. The P2P of the STE is visible in Figure 9 and it is evident that for this combination of parameters the triple contact zone is almost absent. As stated, removing material from the flanks shortens the contact path, effectively reducing the contact ratio of the gears. In this case however with this set of modifications the effective contact ratio becomes very close to 2, minimizing the variation of the STE. The same cannot be said of the misaligned case in the same figure, which still shows severe fluctuations. This modification however has still also beneficial effects on the contact pressures visible in Figure 10. In the rigid case almost the entirety of the flank experiences similar

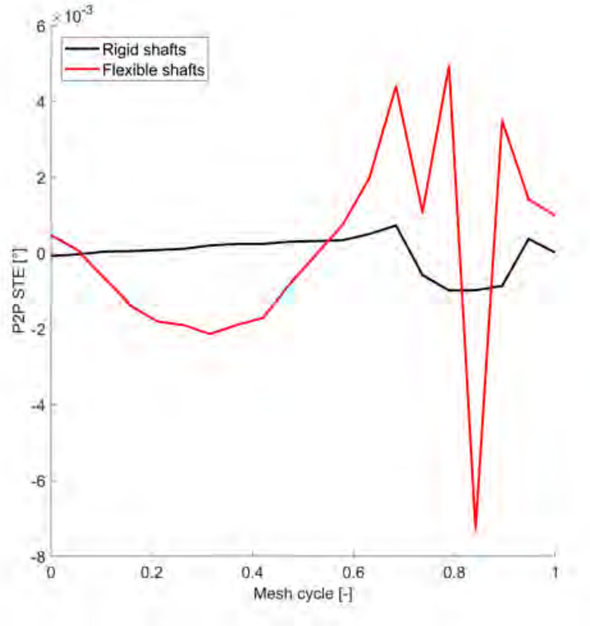

Figure 5 STE comparison with and without misalignment, without profile modifications.

pressures, reducing the risks of damages. Considering the misalignment however still causes some tip corner contact to a lower extent, but still in a dangerous way also since some of the material of the flank doesn't experience any pressure and hence doesn't contribute to the load bearing capability of the transmission.

Table 3 Second set of profile modifications, parabolic tip relief and crowning.

Parameter	Pinion	Gear
dCa	$98.5mm$	$182.5mm$
Ca	$7\mu m$	$7\mu m$
$C\beta In$	$5\mu m$	$5\mu m$
$C\beta Fin$	$5\mu m$	$5\mu m$

CONCLUSIONS

In the present work, very flexible shafts were considered in order to highlight the effect of the compliance of those components. The flexibility of the shafts emphasizes the misalignment effect on the contact patch and STE. It is evident that the misalignment defines an increase of the Peak-to-Peak transmission error and a worsening of the contact pressure distribution. The Tooth Profile Modification strategies can mitigate the effect of misalignment, but the most important conclusion of this paper is that the higher the stiffness of the shafts the lower the effect of misalignment due to deflection. A consequence of the investigated parameters is that shafts, as stiff as possible, are one of the most important elements in the gearbox and TPM could be a valuable strategy for reducing the effect of misalignment. In addiction, the proposed strategy proves to be very effective in pre-design phase in order to set gearbox parameters capable of improving the quality of engagement.

References

Abersek, B., Flasker, J. and Glodez, S. (2004), 'Review of mathematical and experimental models for determination of service life of gears', *Engineering Fracture Mechanics* **71**, 439–453.

Bel Mabrouk, I., El Hami, A., Walha, L. and Zghal, B. (2017), 'Dynamic vibrations in wind energy systems: Application to vertical axis wind turbine', *Mechanical Systems and Signal Processing* **85**, 396–414.

Bruzzone, F., Maggi, T., Marcellini, C. and Rosso, C. (2021*a*), '2d nonlinear and non-hertzian gear teeth deflection model for static transmission error calculation', *Mechanism and Machine Theory* **166**, 104471.

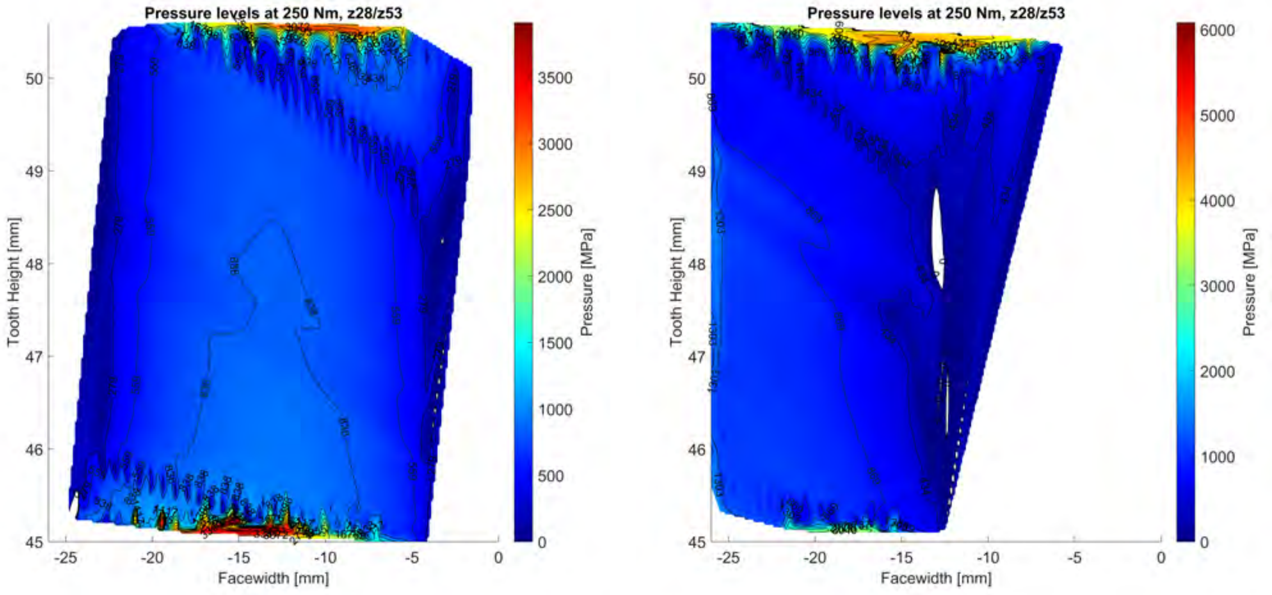

(a) Without misalignment **(b) With misalignment**

Figure 6 Contact pressures along the active flank, without profile modifications

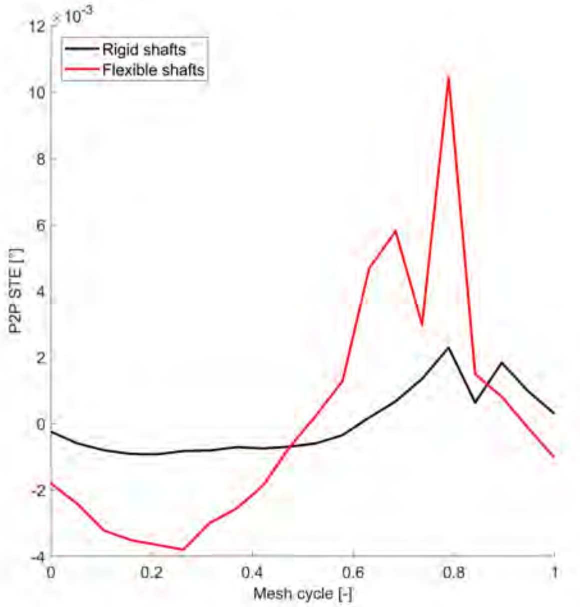

Figure 7 STE comparison with and without misalignment, first set of profile modifications.

Bruzzone, F., Maggi, T., Marcellini, C. and Rosso, C. (2021*b*), 'Gear teeth deflection model for spur gears: Proposal of a 3d nonlinear and non-hertzian approach', *Machines* **9**(10).
URL: *https://www.mdpi.com/2075-1702/9/10/223*

Bruzzone, F. and Rosso, C. (2020), 'Sources of excitation and models for cylindrical gear dynamics: A review', *Machines* **8**(3).
URL: *https://www.mdpi.com/2075-1702/8/3/37*

Chaari, F., Fakhfakh, T. and Haddar, M. (2009), 'Analytical modelling of spur gear tooth crack and influence on gearmesh stiffness', *European Journal of Mechanics-A/Solids* **28**(3), 461–468.

Chi, C. W., Howard, I. and Wang, J. D. (2007), 'An Experimental Investigation of the Static Transmission Error and Tor-

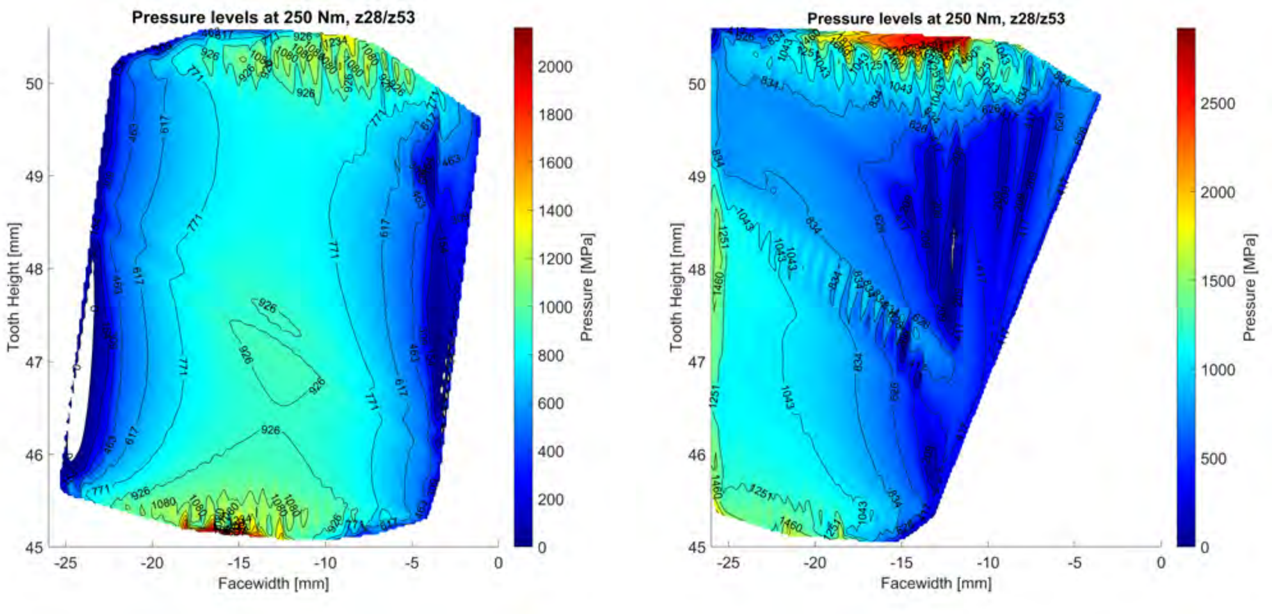

(a) Without misalignment **(b) With misalignment**

Figure 8 Contact pressures along the active flank, first set of profile modifications

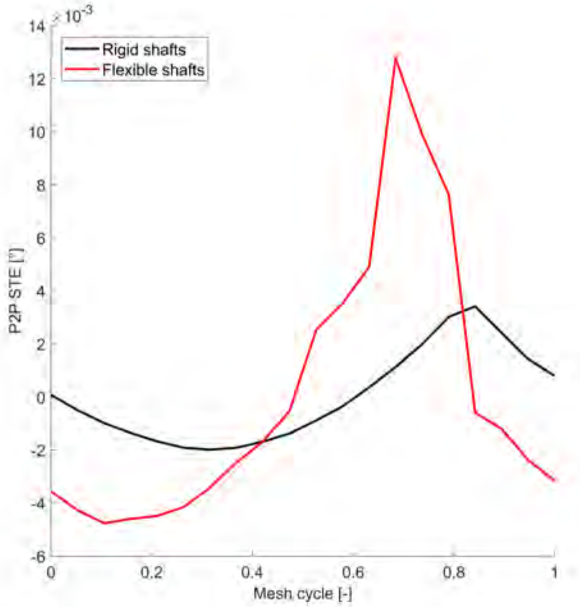

Figure 9 STE comparison with and without misalignment, second set of profile modifications.

sional Mesh Stiffness of Nylon Gears', **Volume 7: 10th International Power Transmission and Gearing Conference**, 207–216.

Cornell, R. W. (1981), 'Compliance and stress sensitivity of spur gear teeth', *Journal of Mechanical Design* **103**, 447–459.

Cornell, R. W. and Westervelt, W. W. (1978), 'Dynamic tooth loads and stressing for high contact ratio spur gears', *Transactions of the American Society of Mechanical Engineers, Journal of Mechanical Design* **100**, 69–76.

Cura, F., Mura, A. and Rosso, C. (2014), 'Investigation about crack propagation paths in thin rim gears', *Frattura e Integrita Strutturale* **30**, 446–453.

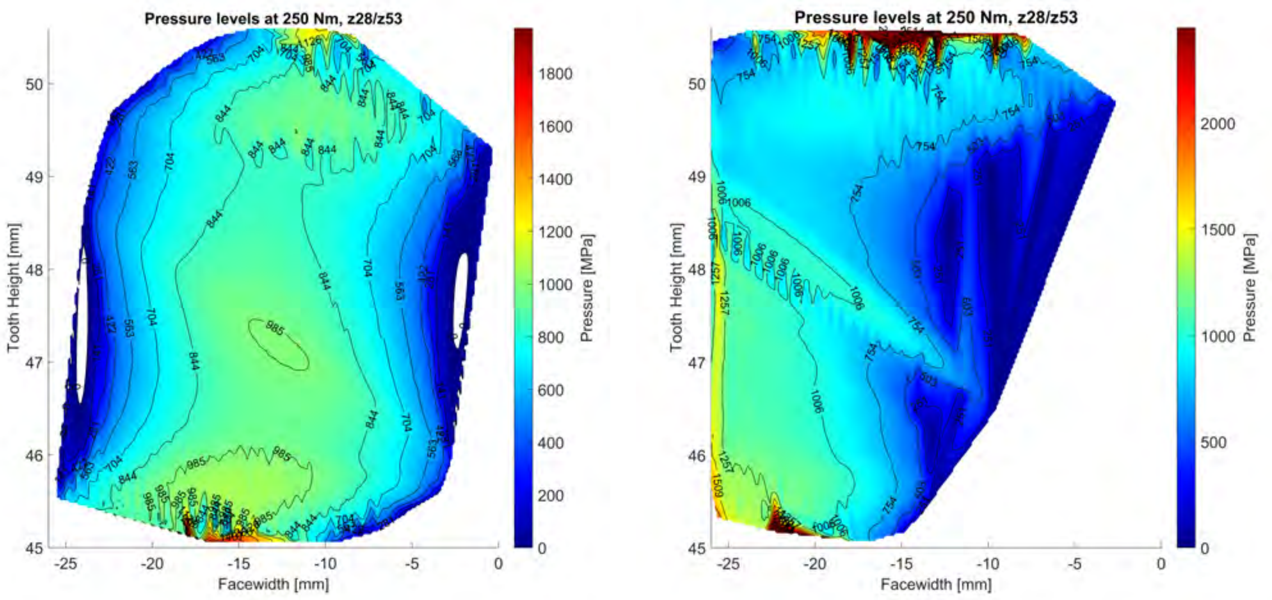

(a) Without misalignment **(b) With misalignment**

Figure 10 Contact pressures along the active flank, second set of profile modifications

Cura, F., Mura, A. and Rosso, C. (2015), 'Effect of rim and web interaction on crack propagation paths in gears by means of xfem technique', *Fatigue and Fracture of Engineering Materials and Structures* pp. 1237–1245.

Deng, G., Nakanishi, T. and Inoue, K. (2003), 'Bending load capacity enhancement using an asymmetric tooth profile', *JSME International Journal Series C* **46**, 1171–1177.

Garambois, P., Donnard, G., Rigaud, E. and Perret-Liaudet, J. (2017), 'Multiphysics coupling between periodic gear mesh excitation and input/output fluctuating torques: Application to a roots vacuum pump', *Journal of Sound and Vibration* **405**, 158—174.

Harris, S. L. (1958), 'Dynamic loads on teeth of spur gears', *Proceedings of the Institution of Mechanical Engineers* **172**, 87–112.

He, S., Gunda, R. and Singh, R. (2007), 'Effect of sliding friction on the dynamics of spur gear pair with realistic time-varying stiffness', *Journal of Sound and Vibration* **301**, 927–949.

Hertz, H. R. (1895), 'On contact between elastic bodies', *Collected Works* **1**.

Hu, W. and Chen, Z. (2003), 'A multi-mesh mpm for simulating the meshing process of spur gears', *Computers and Structures* **81**, 1991–2002.

Inalpolat, M., Handschuh, M. and Kahraman, A. (2015), 'Influence of indexing errors on dynamic response of spur gear pairs', *Mechanical Systems and Signal Processing* **60-61**, 391—405.

Johnson, K. L. (1985), *Contact Mechanics*, Cambridge University Press.

Kadmiri, Y., Perret-Liaudet, J., Rigaud, E., Le Bot, A. and Vary, L. (2011), 'Influence ofmultiharmonics excitation on rattle noise in automotive gearboxes', *Advances in Acoustics and Vibration* **2011**, 659797.

Kalker, J. J. (1990), *Three-Dimensional Elastic Bodies in Rolling Contact*, Springer Netherlands.

Kubo, A., Kiyono, S. and Fujino, M. (1986), 'On analysis and prediction of machine vibration caused by gear meshing (1st report, nature of gear vibration and the total vibrational excitation)', *Bullettin of the Japan Society of Mechanical Engineers* **29**, 4424–4429.

Lin, T., Ou, H. and Li, R. (2007), 'A finite element method for 3d static and dynamic contact/impact analysis of gear drives', *Computer Methods in Applied Mechanics and Engineering* **196**, 1716–1728.

Litvin, F. L. (1994), *Gear geometry and applied theory*, P. T. R. Prentice Hall.

Ma, H., Pang, X., Feng, R. J., Zeng, J. and Wen, B. C. (2015), 'Improved time-varying mesh stiffness model of cracked spur gears', *Engineering Failure Analysis* **55**, 271–287.

Nikolic, V., Dolicanin, C. and Dimitrijevic, D. (2012), 'Dynamic model for the stress and strain state analysis of a spur gear transmission', *Journal of Mechanical Engineering* **58**, 56–67.

Ozguven, H. N. and Houser, D. R. (1988), 'Mathematical models used in gear dynamics - a review', *Journal of Sound and Vibration* **121**, 383–411.

Parker, R. G., Vijayakar, S. M. and Imajo, T. (2000), 'Non-linear dynamic response of a spur gear pair: Modelling and experimental comparisons', *Journal of Sound and Vibration* **237**, 435–455.

Pedersen, N. L. and Jorgenses, M. F. (2014), 'On gear tooth stiffness evaluation', *Computers and Structures* **135**, 109–117.

Prasil, L. and Mackerle, J. (2008), 'Finite element analyses and simulations of gears and gear drives a bibliography 1997-2006', *International Journal for Computer-Aided Engineering and Software* **25**, 196–219.

Qin, W. and Guan, C. (2014), 'An investigation of contact stresses and crack initiation in spur gears based on finite element dynamics analysis', *International Journal of Mechanical Sciences* **83**, 96–103.

Raghuwanshi, N. K. and Parey, A. (2016), 'Experimental measurement of gear mesh stiffness of cracked spur gear by strain gauge technique', *Measurement* **86**, 266–275.

Raghuwanshi, N. K. and Parey, A. (2018), 'Experimental measurement of mesh stiffness by laser displacement sensor technique', *Measurement* **128**, 63–70.

Sato, T., Umezawa, K. and Ishikawa, J. (1983), 'Effects of contact ratio and profile correction on gear rotational vibration', *Bullettin of the Japan Society of Mechanical Engineers* **26**, 2010–2016.

Umezawa, K., Ajima, T. and Houhoh, H. (1986), 'Vibration of three axes gear system (in japanese)', *Bullettin of the Japan Society of Mechanical Engineers* **29**, 950–957.

Umezawa, K., Sato, T. and Ishikawa, J. (1984), 'Simulation on rotational vibration of spur gears', *Bullettin of the Japan Society of Mechanical Engineers* **27**, 102–109.

Ural, A., Heber, G., Wawrzynek, P. A., Ingraffea, A. R., Lewicki, D. G. and Neto, J. B. (2005), 'Three-dimensional, parallel, finite element simulation of fatigue crack growth in a spiral bevel pinion gear', *Engineering Fracture Mechanics* **72**(8), 1148–1170.

Wang, J. D. and Howard, I. M. (2006), 'Error analysis of finite element modeling of involute spur gears', *Journal of Mechanical Design* **128**, 90–97.

Wang, Q. and Zhang, Y. (2017), 'A model for analyzing stiffness and stress in a helical gear pair with tooth profile errors', *Journal of Vibration and Control* **23**, 272–289.

Weber, C. (1949), 'The deformation of load gears and the effect on their load-carrying capacity. technical report n.3', *British Department of Scientific and Industrial Research* .

Weber, C. and Banaschek, K. (1953), *Formänderung und profilrücknahme bei gerad-und schragverzahnten antriebstechnik*, F. Vieweg.

Wei, J., Sun, W. and Wang, L. (2011), 'Effect of flank deviation on load distributions for helical gear', *Journal of Mechanical Science and Technology* **25**, 1781–1789.

Wriggers, P. (2002), *Computational contact mechanics*, Springer.

Y. Tesfahuneng, A., Rosa, F. and Gorca, C. (2010), 'The effects of the shape of tooth profile modifications on the transmission error, bending and contact stress of spur gears', *Proceedings of the Institution of Mechanical Engineering Part C: Journal of Mechanical Engineering Science* **224**, 1749–1758.

Yang, D. C. H. and Lin, J. Y. (1986), 'Hertzian damping, tooth friction and bending elasticity in gear impact dynamics', *Transactions of the American Society of Mechanical Engineers, Journal of Mechanisms, Transmissions, and Automation in Design* **109**, 189–196.

Zhang, Y., Wang, Q., Ma, H., Huang, J. and Zhao, C. (2013), 'Dynamic analysis of three-dimensional helical geared rotor system with geometric eccentricity', *Journal of Mechanical Science and Technology* **27**, 3231—3242.